ARTICLE

H-atom Dissociation Channels in Ultraviolet Photochemistry of m-Pyridyl Radical

Michael Lucas[a], Jasmine Minor[a], Jingsong Zhang[a,c*], Christopher Brazier[b]

a. Department of Chemistry, University of California, Riverside, CA 92521, USA
b. Department of Chemistry and Biochemistry, California State University, Long Beach, CA 90840, USA
c. Air Pollution Research Center, University of California, Riverside, CA 92521, USA

(Dated: Received on September 8, 2014; Accepted on September 30, 2014)

The H atom production channels in the ultraviolet (UV) photochemistry of m-pyridyl radical (m-C_5H_4N) were investigated at excitation wavelengths from 224 nm to 248 nm by high-n Rydberg atom time-of-flight (HRTOF) technique. The photofragment yield (PFY) spectrum of the H atoms indicates a broad UV absorption feature near 234 nm. The product kinetic energy release is small; the average product kinetic energy at the wavelengths from 224 nm to 248 nm is 0.12 to 0.19 of the maximum excess energy (assuming the lowest energy product channel, H+cyanovinylacetylene). The product kinetic energy distributions are consistent with the H+cyanovinylacetylene, H+3,4-pyridyne, and H+2,3-pyridyne product channels, with H+cyanovinylacetylene as the main H-loss channel. The angular distributions of the H-atom products are isotropic. After the UV electronic excitation, the m-pyridyl radical undergoes internal conversion to the ground electronic state and then unimolecular dissociation to the H+cyanovinylacetylene, H+3,4-pyridyne, and H+2,3-pyridyne products. The dissociation mechanism of the m-pyridyl radical is similar to that of the o-pyridyl radical reported in the early study.

Key words: Photolysis, Photofragment, Pyridyl, Pyridine, Decomposition, Excited state

I. INTRODUCTION

Combustion of nitrogen containing aromatic fuels is frequently modeled on behavior of the simplest member of this group, pyridine [1]. The first step in decomposition of pyridine usually involves one of the three isomeric pyridyl radicals (C_5H_4N), o-, m-, and p-pyridyl [2−9]. We have recently published an analysis of the ultraviolet (UV) photolysis of the lowest energy o-pyridyl isomer [10], and we report here the corresponding results for m-pyridyl.

Thermal dissociation of the pyridyl radicals has been investigated in the pyrolysis of pyridine at elevated temperature [2−9]. The initial step in pyridine decomposition is C−H bond dissociation to o-pyridyl [4], more favored than the p- and m-pyridyl which are 4.4 and 5.7 kcal/mol higher in energy, respectively [11]. The thermal decomposition experiments suggested that dissociation of the o- and m-pyridyl proceeded via C−N bond fission to open-chain radicals, ·CH=CH−CH=CH−C≡N and HC≡C−CH=CH−CH=N·, respectively, which then lost C_2H_2, HCN, and H atom [4, 6−8]. The decomposition products of o-pyridyl and m-pyridyl are similar, but with an increase production of C_2H_2 from o-pyridyl versus HCN from m-pyridyl [4, 7, 8]. The dissociation of the o-, m-, and p-pyridyl radicals were also investigated by neutralization-reionization mass spectrometry [12]. It was observed that the pyridyl radicals decomposed by losing either C_2H_2 or HCN, and small H-loss channels to produce 2,3-pyridyne in o-pyridyl and 3,4-pyridyne in m-pyridyl were also suggested [12].

Theoretical investigations of the unimolecular decomposition of m-pyridyl indicated that the initial dissociation step involves C−N bond cleavage to form the open-chain radical (I), HC≡C−CH=CH−CH=N· [11, 13, 14]. The energetics and unimolecular dissociation pathways of m-pyridyl derived from the calculations by Liu *et al.* [11] are shown in Fig.1. The open-chain radical (I) can dissociate via C−H cleavage to H+cyanovinylacetylene (HC≡C−CH=CH−C≡N), the lowest energy channel, or via C−C bond dissociation to HCN+·CH=CH−C≡CH, the second lowest energy channel [11, 13, 14]. Two direct C−H dissociations, H+3,4-pyridyne and H+2,3-pyridyne, are at higher energies. C−C bond fission decyclization is a high energy pathway of m-pyridyl, giving rise to an open-chain radical, ·CH=CH−N=CH−C≡CH, which could dissociate to H+ethynamine (HC≡CN=CHC≡CH), the highest e-

*Author to whom correspondence should be addressed. E-mail: jingsong.zhang@ucr.edu.

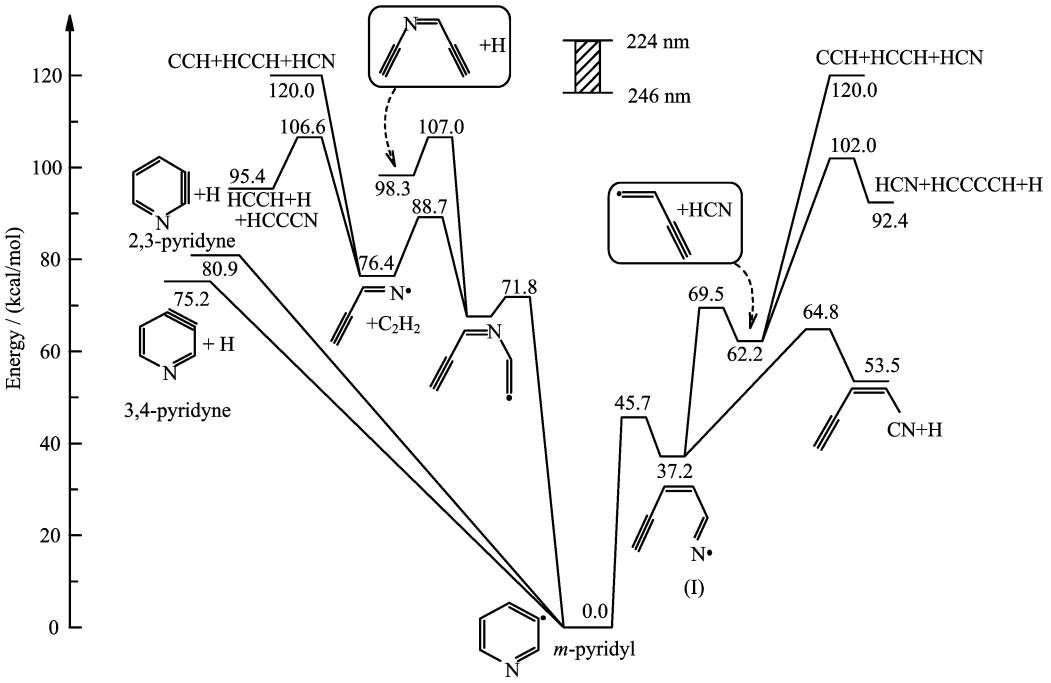

FIG. 1 Energetics of the *m*-pyridyl dissociation pathways, derived from the theoretical work by Liu *et al.* [11].

nergy H-atom loss channel [11, 13, 14]. The energies of the H-atom production and C−C bond dissociation channels of *m*-pyridyl are as follows [11]:

$$m\text{-}C_5H_4N \rightarrow H + HC \equiv C - CH = CH - C \equiv N \quad (1)$$
$$\Delta H_{rxn,0} = 53.5 \text{ kcal/mol}$$
$$\rightarrow H + \text{3,4-pyridyne} \quad (2)$$
$$\Delta H_{rxn,0} = 75.2 \text{ kcal/mol}$$
$$\rightarrow H + \text{2,3-pyridyne} \quad (3)$$
$$\Delta H_{rxn,0} = 80.9 \text{ kcal/mol}$$
$$\rightarrow H + HC \equiv CN = CHC \equiv CH \quad (4)$$
$$\Delta H_{rxn,0} = 98.3 \text{ kcal/mol}$$
$$\rightarrow HCN + \cdot CH = CH - C \equiv CH \quad (5)$$
$$\Delta H_{rxn,0} = 62.2 \text{ kcal/mol}$$
$$\rightarrow C_2H_2 + \cdot N = CH - CCH \quad (6)$$
$$\Delta H_{rxn,0} = 76.4 \text{ kcal/mol}$$

As with *o*-pyridyl limited information is available for the electronically excited states and photodissociation of *m*-pyridyl [10, 15, 16]. UV photochemistry of the pyridyl radicals at 240−380 nm wavelengths was studied in argon matrices using electron-spin resonance (ESR) detection [16]. It was found that the *o*- and *m*-pyridyl radical rupture the aromatic rings via C−N bond fission and form the open-chain radicals, ·CH=CH−CH=C−C≡N and HC≡C−CH=CH−CH=N·, respectively. The HC≡C−CH=CH−CH=N· radical from *m*-pyridyl could further loss HCN under the UV irradiation [16]. For both pyridyl radicals the UV transition likely involves an n(N)→π^* electronic excitation [16]. In our previous work on the UV photodissociation of *o*-pyridyl, a broad absorption feature was observed between 224 and 246 nm [10]. The UV photodissociation of *o*-pyridyl took place via internal conversion and then unimolecular decomposition of the hot radical on the ground electronic state. The products kinetic energy distributions indicated that the UV photolysis of *o*-pyridyl mainly produces the lowest energy products, cyanovinylacelylene and hydrogen, consistent with the C−N bond fission and open-chain radical pathway.

In this work, we investigated the UV photodissociation dynamics of the corresponding jet-cooled *m*-pyridyl radical in the same UV wavelength region. Direct observation of the H-atom products as a function of photolysis wavelength generated the photofragment yield (PFY) spectrum, showing the UV absorption of *m*-pyridyl. The time-of-flight (TOF) spectra of the H-atom products were measured, and the product kinetic distributions were derived, providing information on the decomposition mechanism. The angular distributions of the H-atom products were also measured. The photodissociation dynamics and mechanisms of the *o*-pyridyl and *m*-pyridyl isomers are then compared.

II. EXPERIMENTS

The high-*n* Rydberg atom time-of-flight (HRTOF) technique and experimental apparatus have been presented in previous studies [17−21] and were identical to those for the *o*-pyridyl study [10]. A ∼2% mixture

DOI:10.1063/1674-0068/27/06/621-627

of 3-chloro-pyridine or 3-bromo-pyridine (MP Biomedicals) in He (at a pressure of ∼120 kPa) was expanded from a pulsed valve (General Valve, Series 9) and photolyzed with an ArF excimer laser at 193 nm to generate the *m*-pyridyl radical beam. The 3-chloro-pyridine or 3-bromo-pyridine sample was kept in a glass bubbler immersed in a variable temperature water bath. The *m*-pyridyl radical beam was characterized by photoionization TOF mass spectrometry (TOFMS) at 121.6 nm. The *m*-pyridyl radicals were photolyzed by the tunable UV laser radiation (at 224−248 nm, <1.0 mJ/pulse, linewidth ∼0.3 cm^{-1}). The polarization of the photolysis laser radiation could be rotated by an achromatic $\lambda/2$ plate for product angular distribution measurements. The H atom products in the *m*-pyridyl photodissociation were probed by a two-color resonant excitation process, first from 1^2S to 2^2P via the 121.6-nm Lyman-α transition and second to a high-*n* Rydberg state by 366.4 nm UV radiation. A microchannel plate (MCP) detector was installed perpendicularly to the molecular beam and collected a small portion of the H-atom products flying with their nascent velocities in this direction. The metastable Rydberg H atoms arriving at the MCP detector were field-ionized and detected. The flight length was calibrated to be 37.12 cm. The H-atom TOF spectra were accumulated by a multichannel scaler, typically from 100 K to 350 K laser firings. To minimize multi-photon signals from the residual precursor molecules and the radicals, the H-atom TOF spectra were measured at photolysis power <0.5 mJ/pulse as had been done for *o*-pyridyl. The time profile of the H-atom production was studied by measuring the HRTOF signals as a function of the photolysis-probe laser delay time. The H-atom product from *m*-pyridyl was formed within the overlap of the photolysis and probe laser pulses, whose temporal resolution was restricted by the 8-ns laser pulse.

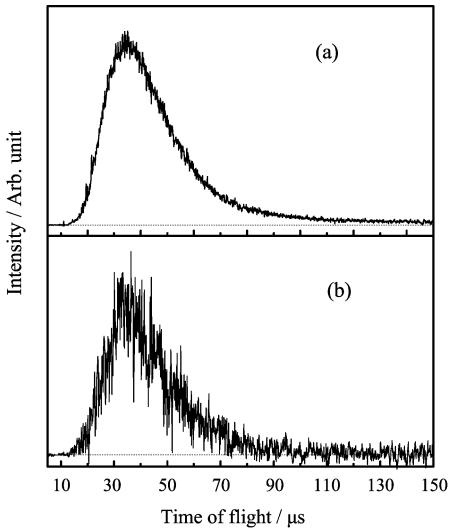

FIG. 2 Net H-atom TOF spectra in photolysis of jet-cooled *m*-pyridyl radical at 232 nm, using (a) 3-chloropyridine and (b) 3-bromopyridine precursors. The photolysis laser power was 0.3−0.5 mJ/pulse.

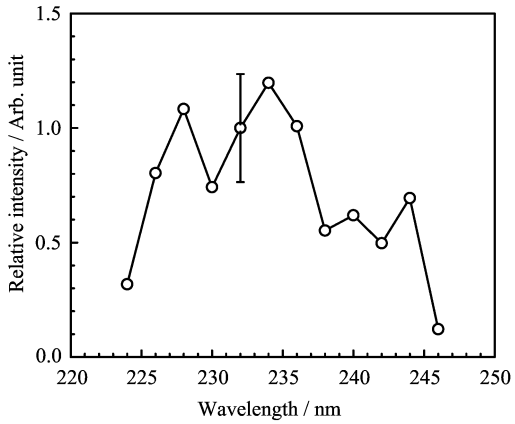

FIG. 3 H-atom PFY spectrum as a function of photolysis excitation energy in the region of 224−246 nm. The open circles represent integrated HRTOF signals using the 3-chloropyridine precursor. The error bar indicates 1σ uncertainty based on multiple measurement statistics.

III. RESULTS

The HRTOF spectra of the H-atom products from the photolysis of *m*-pyridyl were taken at UV wavelengths from 224 nm to 248 nm. To remove background signals from the residual precursor molecules, the TOF spectra were recorded with the 193-nm photolysis laser on and off. The H-atom TOF spectra reported are the net results of the 193-nm photolysis-on spectra minus the 193-nm photolysis-off spectra. The net H-atom TOF spectra were obtained with both 3-chloro-pyridine and 3-bromo-pyridine, showing similar spectra (Fig.2). The HRTOF spectrum using the 3-bromo-pyridine precursor had a poorer signal-to-noise ratio, mainly due to the fewer number of signal averaging using 3-bromo-pyridine (which has a lower vapor pressure). In order to get a similar concentration (∼2%) of the 3-chloro-pyridyne and 3-bromo-pyridine molecules in the gas phase, higher bath temperature had to be used for 3-bromo-pyridine, which increased the risk that the precursor molecules condensed in the pulsed valve thus blocking the nozzle.

The H-atom TOF spectra were measured at 2-nm intervals over the 224−246 nm range. The integrated intensities of the net TOF spectra constitute the PFY (action) spectrum of *m*-pyridyl and are shown in Fig.3. In order to normalize the experimental conditions in the action spectrum, the H-atom product signals at 232 nm were chosen as a reference and taken between every 2−3 measurements at other wavelengths. The integrated H-atom product signals were normalized with the UV photolysis laser power and scaled to those at 232 nm. The PFY spectrum is broad with the greatest intensity in

DOI:10.1063/1674-0068/27/06/621-627

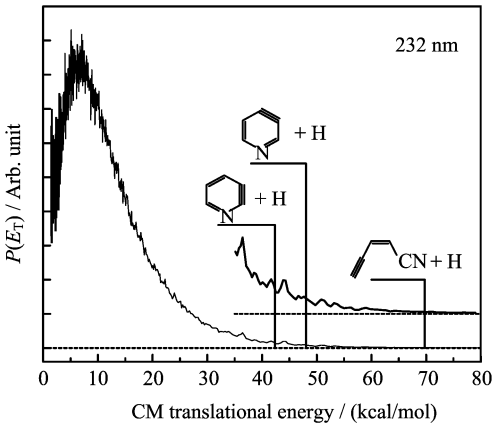

FIG. 4 $P(E_{\rm T})$ distribution of the H-atom loss channel of the m-pyridyl radical photolysis at 232 nm, derived from direct conversion of the H-atom TOF spectrum in Fig.2(a). The vertical lines indicate the maximum kinetic energies of the three H-atom production channels, H+cyanovinylacetylene, H+3,4-pyridyne, and H+2,3-pyridyne, from Liu *et al.* [11].

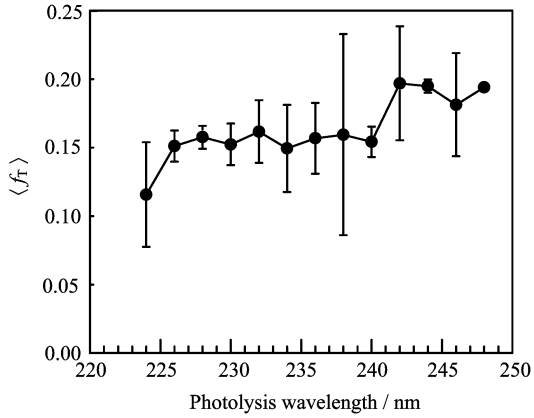

FIG. 5 $\langle f_{\rm T}\rangle$ versus photolysis wavelength in the UV photolysis of the m-pyridyl radical. The average kinetic energies are calculated from the measured $P(E_{\rm T})$ distributions. The total available energy is based on the dissociation energy of the lowest energy product channel, H+cyanovinylacetylene. The error bars represent 95% confidence limit.

the 226−236 nm region. The point-to-point variations in the action spectrum are possibly from fluctuation of the low signals, but sharper absorption features could not be ruled out.

The products center-of-mass (CM) translational energy distributions, $P(E_{\rm T})$, were derived from the net H-atom TOF spectra at various photolysis wavelengths using direct conversion [18, 22]. The resulting translational energy profile of the m-pyridyl photodissociation at 232 nm is shown in Fig.4. Also shown are the maximum available energies derived from the calculations by Liu *et al.* [11], for the three possible H-loss product channels, H+cyanovinylacetylene (69.7 kcal/mol), H+3,4-pyridyne (48.0 kcal/mol), and H+2,3-pyridyne (42.3 kcal/mol).

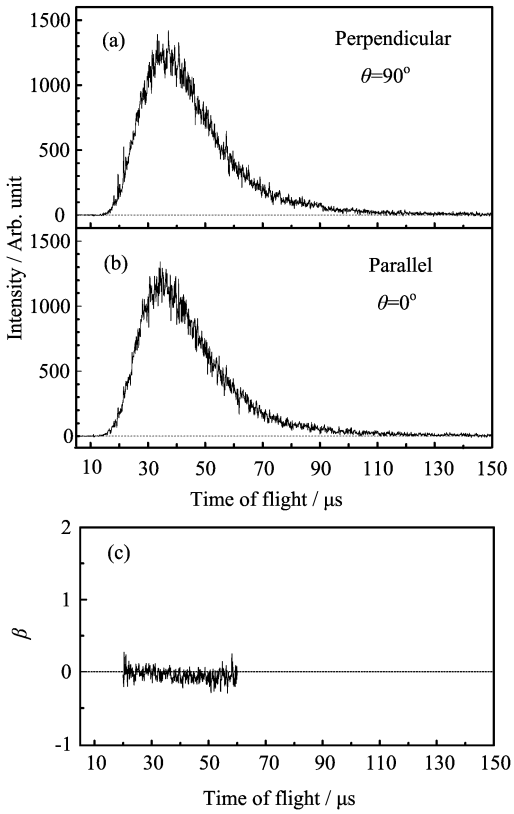

FIG. 6 H-atom product angular distribution. HRTOF spectra of photolysis of m-pyridyl at 232 nm, with the polarization of the photolysis radiation (a) perpendicular (θ=90°) and (b) parallel (θ=0°) to the flight axis. The signals are normalized with the photolysis power and laser shots. (c) Anisotropy parameter β as a function of H-atom time of flight. The β parameter stays near zero for an isotropic angular distribution.

The $P(E_{\rm T})$ distribution is broad and featureless. It has a low-energy peak near ∼7 kcal/mol and reaches the maximum excess energy of the H+cyanovinylacetylene products. The average kinetic energy release is low, 11.3 kcal/mol at 232 nm. This corresponds to a fraction of the average kinetic energy in the maximum excess energy (assuming the H+cyanovinylacetylene channel), $\langle f_{\rm T}\rangle$, of 0.16 at 232 nm. At the photolysis wavelengths from 224 nm to 248 nm, the $\langle f_{\rm T}\rangle$ values are in the range of 0.12−0.19, with a weighted average of 0.18 (Fig.5). Note that these $\langle f_{\rm T}\rangle$ values based on the H+cyanovinylacetylene product channel are the lower limits. The $\langle f_{\rm T}\rangle$ values would be higher if other product channels contribute. If 3,4-pyridyne+H is assumed as the only product channel, the $\langle f_{\rm T}\rangle$ values would be in the range of 0.16−0.30 with an average of 0.26, and for 2,3-pyridyne+H, in the range of 0.18 to 0.35 and an average of 0.30.

The H-atom product angular distributions from the photolysis of m-pyridyl were measured with linearly polarized UV laser radiation. The product angular distri-

DOI:10.1063/1674-0068/27/06/621-627

butions at 232 nm are shown in Fig.6. The photolysis radiation was linearly polarized parallel or perpendicular to the flight axis. The H-atom TOF spectra were identical for both polarizations, indicating an isotropic angular distribution (anisotropy parameter $\beta \approx 0$).

IV. DISCUSSION

The photochemistry of the *m*-pyridyl radical was examined at the wavelengths from 224 nm to 248 nm. The HRTOF spectra directly revealed the H-atom loss channel of *m*-pyridyl. The H-atom PFY spectrum shows a broad feature that peaks near 234 nm. If H-atom loss is the dominant product channel, the PFY spectrum could represent the UV absorption spectrum of *m*-pyridyl. The PFY spectrum is consistent with the UV photochemistry of the pyridyl radicals in the argon matrices, which was observed in the wavelength range of 240−380 nm and assumed to be from the n(N)$\rightarrow\pi^*$ transition [16]. The UV absorption of *m*-pyridyl is similar to that of the isoelectronic phenyl radical, peaking around 235 nm in the same region [21, 23]. The *m*-pyridyl and *o*-pyridyl spectra both have broad features in the same region; however, the intensity in the *m*-pyridyl spectrum decreases at wavelengths shorter than 225 nm, different from that of *o*-pyridyl [10]. Although sharper features in the action spectrum could not be ruled out due to the current experimental limitation, a broad UV absorption feature of *m*-pyridyl would imply a fast decay of the electronic excited state, possibly to the ground state via internal conversion, as in the *o*-pyridyl radical [10] and the phenyl radical [21, 24].

The $P(E_T)$ values of the H-atom dissociation channels of *m*-pyridyl are all similar in the photolysis wavelength region of 224−248 nm (Fig.4). The $P(E_T)$ values are broad, with a small peak and the maximum energy extended to the onset of the H+cyanovinylacetylene channel. The $P(E_T)$ values indicate non-repulsive kinetic energy disposal. The $\langle f_T \rangle$ value is small, varying from 0.12 to 0.19 in the region of 224 nm to 248 nm (based on the total excess energy of the cyanovinylacetylene+H channel) (Fig.5). The $P(E_T)$ distributions of *m*-pyridyl and *o*-pyridyl have essentially the same shape, and their $\langle f_T \rangle$ values are similar, with the same average value of 0.18 at the photolysis wavelengths from 224 nm to 248 nm [10]. The broad shape and low-energy peak of the $P(E_T)$ distributions are characteristic of a statistical energy disposal in the unimolecular decomposition of a polyatomics. The $P(E_T)$ distributions are consistent with a mechanism of hot radical decomposition; the pyridyl radical first decays from the electronic excited state to vibrationally hot ground electronic state via internal conversion and then undergoes unimolecular dissociation.

The previous UV photochemistry study of the *m*-pyridyl radical in the argon matrices using ESR suggested that the UV photodissociation of *m*-pyridyl proceed via the open-chain radical (I) [16]. The theoretical studies also indicated that the *m*-pyridyl radical first undergoes C−N bond fission and ring opening to the open-chain radical (I), HC≡C-CH=CH−CH=N·, and then dissociates to H+cyanovinylacetylene via C−H bond cleavage and HCN+·CH=CH−CCH via C−C bond dissociation (Fig.1) [11, 13, 14]. While the previous experimental studies on the thermal dissociation of pyridine proposed HCN and ·CH=CH−CCH as the major products from *m*-pyridyl [4, 6], our current work directly observes the H-atom products and the kinetic energy distribution. The H-loss products $P(E_T)$ distribution of the *m*-pyridyl photodissociation at 232 nm extends to the energy threshold of the lowest energy products, directly showing the H+cyanovinylacetylene products (Fig.4). The smooth $P(E_T)$ distribution could also contain contributions from the higher energy H+3,4-pyridyne and H+2,3-pyridyne channels. However, the $P(E_T)$ distribution shows no obvious profile change around the onsets of the 3,4-pyridyne+H and 2,3-pyridyne+H channels (Fig.4), suggesting no major contributions from these two channels.

If cyanovinylacetylene+H is assumed as the only channel, the observed product translational energy release corresponds to the average $\langle f_T \rangle$ value of 0.18 in the region of 224 nm to 248 nm photolysis wavelengths, while the $\langle f_T \rangle$ value is 0.26 for the 3,4-pyridyne+H channel and 0.30 for the 2,3-pyridyne+H channel, respectively. The $\langle f_T \rangle$ values assuming the exclusive 3,4-pyridyne+H or 2,3-pyridyne+H product channel seem to be too high for these two simple bond fission channels that do not have an exit barrier; this would also suggest that these two higher energy channels are not the major channels. The ∼7 kcal/mol peak in the $P(E_T)$ is consistent with the exit barrier of 11 kcal/mol for dissociation of the open-chain radical (I) to cyanovinylacetylene+H (Fig.1) [11]. Thus it is likely that the cyanovinylacetylene+H channel is the main H-loss dissociation channel for its considerably lower energy, while the H+3,4-pyridyne and H+2,3-pyridyne channels could still contribute. The fourth, highest energy H-loss channel, H+HC≡CN=CHC≡CH, via the C−C bond fission intermediate ·CH=CH−N=CH−C≡CH is unlikely to contribute in the *m*-pyridyl photolysis for its high energy threshold and reaction barrier. Our conclusion of the H+cyanovinylacetylene channel as the main H-loss channel agrees with the theoretical studies [11, 13, 14] and is similar to that of the *o*-pyridyl radical [10]. The HRTOF technique in this study was not sensitive to the HCN and ·CH=CH−CCH products of *m*-pyridyl. This C−C bond dissociation pathway, being the second lowest energy channel, could be competitive with the cyanovinylacetylene+H products [4, 6, 11, 13, 14].

The H-atom product angular distribution in the 232 nm photolysis of *m*-pyridyl is isotropic (Fig.6), similar to *o*-pyridyl. The isotropic distribution indicates that the time scale of *m*-pyridyl dissociation is longer than its rotational period (∼ps), which agrees with the

DOI:10.1063/1674-0068/27/06/621-627

non-repulsive, small product kinetic energy disposal in the H-atom dissociation. The isotropic angular distribution and dissociation timescale are also consistent with the hot radical unimolecular decomposition mechanism following internal conversion.

The dissociation of phenyl, *o*-pyridyl, and *m*-pyridyl, three isoelectronic aromatic radicals are compared here. The *m*-pyridyl and *o*-pyridyl radical can undergo ring-opening decyclization via C−N bond cleavage (more favorable than the C−C bond fission), but form two different isoelectronic open-chain radical intermediates, radical (I) HC≡C−CH=CH−CH=N· and the cyano radical ·HC=CH−CH=CH−C≡N, respectively [4, 6, 11, 13, 14]. The radical (I) from *m*-pyridyl and the cyano radical from *o*-pyridyl could dissociate via C−H bond dissociation to the same linear products H+HC≡C−CH=CH−C≡N (the lowest energy product channel for both pyridyl isomers), which is considered as the main H-loss product channel in this study of *m*-pyridyl and in the earlier study of *o*-pyridyl [10]. The second lowest energy product channel of *m*- and *o*-pyridyl are C−C bond dissociation of the open-chain radical intermediates, HCN+·CH=CH−C≡CH (Fig.1) and C_2H_2+·CH=CH−C≡N, respectively (Fig.1) [4, 6, 11, 13, 14]. Both pyridyl radicals can also undergo simple C−H bond dissociation to form cyclic pyridyne products in higher energy pathways, but due to the difference in the radical sites, *o*-pyridyl has only one such product channel, H+2,3-pyridyne, while *m*-pyridyl has two, H+3,4-pyridyne and H+2,3-pyridyne [11, 13, 14]. In the phenyl radical, formation of H+*o*-benzyne products from direct H-atom loss from the aromatic ring is the lowest energy dissociation channel [25−27] and the main decomposition pathway, as shown in the UV photolysis studies of phenyl around 240 nm [21, 24]. The open-chain pathways of phenyl, C−C bond decyclization to an open-chain intermediate, ·CH=CH−CH=CH−C≡CH (*l*-C_6H_5) and subsequent decompositions to H+HC≡C−CH=CH−C≡CH (*l*-C_6H_4) and C_2H_2+·CH=CH−C≡CH (*n*-C_4H_3), are in higher energies [25−27]. In comparing the pyridyl and phenyl radicals, the C−N bond decyclization of *m*- and *o*-pyridyl to the open-chain radicals require considerably lower energy than the C−C bond decyclization of phenyl to *l*-C_6H_5 [11, 13, 14, 27]. The H-atom loss (H+cyanovinylacetylene) and C−C breaking (HCN+·CH=CH-C≡CH and C_2H_2+cyanovinyl radical) of *m*-pyridyl and *o*-pyridyl via the open radical intermediates are lower in energy than the direct C−H bond dissociation to the cyclic 3,4-pyridyne or 2,3-pyridyne products. Consequently, H+cyanovinylacetylene is the main H-atom loss channel for both *m*- and *o*-pyridyl. In the phenyl radical, the energy for C−C bond ring-opening is significantly higher, placing the *l*-C_6H_4+H and C_2H_2+*n*-C_4H_3 product channels above H+*o*-benzyne and thus making direct C−H bond breaking on the aromatic ring the main pathway in phenyl. Noticeably, in going from the phenyl to the pyridyl radicals where a C atom is substituted with an N atom, the aromatic ring is significantly weakened, and the dissociation pathways via the C−N cleavage ring-opening intermediates are energetically more favorable. This change in energy associated with the structural variation has altered the dissociation pathways of the phenyl radical and the two pyridyl radicals.

V. CONCLUSION

The H-atom loss channels in the UV photochemistry of the *m*-pyridyl radical were investigated at the photolysis wavelengths from 224 nm to 248 nm. The H-atom PFY spectrum of *m*-pyridyl reveals a broad UV absorption of the *m*-pyridyl radical in the region of 224−248 nm. The product kinetic energy release of the H-atom production channels is small, with the $\langle f_T \rangle$ values in the range of 0.12−0.19 in the 224−248 nm region (assuming the lowest energy dissociation channel, H+cyanovinylacetylene). The $P(E_T)$ distributions are consistent with the H+cyanovinylacetylene, H+3,4-pyridyne, and H+2,3-pyridyne product channels, with H+cyanovinylacetylene being more important. The product angular distribution of the H-atom product is isotropic. The dissociation mechanisms of *m*-pyridyl and *o*-pyridyl are very similar; both are unimolecular decomposition of hot radicals in the highly vibrationally excited ground electronic state following internal conversion of the electronically excited radicals.

VI. ACKNOWLEDGMENTS

This work was supported by the US National Science Foundation (CHE-1214157). Jasmine Minor acknowledges the support from the UC Riverside HSI-STEM Summer Bridge to Research Program and the Summer Research in Science and Engineering [RISE] Program.

[1] J. F. Unsworth, D. J. Barratt, and P. T. Roberts, *Coal Quality and Combustion Performance*, Amsterdam: Elsevier Science Publishers, (1991).
[2] T. J. Houser, M. E. McCarville, and T. Biftu, Int. J. Chem. Kinet. **12**, 555 (1980).
[3] H. I. Leidreiter and H. G. Wagner, Zeitschrift Fur Physikalische Chemie Neue Folge **153**, 99 (1987).
[4] J. C. Mackie, M. B. Colket, and P. F. Nelson, J. Phys. Chem. **94**, 4099 (1990).
[5] V. R. Morris, S. C. Bhatia, A. W. Stelson, and J. H. Hall, Energy Fuels **5**, 126 (1991).
[6] E. Ikeda and J. C. Mackie, J. Anal. Appl. Pyroly. **34**, 47 (1995).
[7] J. H. Kiefer, Q. Zhang, R. D. Kern, J. Yao, and B. Jursic, J. Phys. Chem. A **101**, 7061 (1997).
[8] N. R. Hore and D. K. Russell, J. Chem. Soc. Perkin Transact. **2**, 269 (1998).

DOI:10.1063/1674-0068/27/06/621-627

[9] H. U. R. Memon, K. D. Bartle, J. M. Taylor, and A. Williams, Inter. J. Energy Res. **24**, 1141 (2000).
[10] M. Lucas, J. Minor, J. S. Zhang, and C. Brazier, J. Phys. Chem. A **117**, 12138 (2013).
[11] R. F. Liu, T. T. S. Huang, J. Tittle, and D. H. Xia, J. Phys. Chem. A **104**, 8368 (2000).
[12] F. Turecek, J. K. Wolken, and M. Sadilek, European Mass Spectrometry **4**, 321 (1998).
[13] Y. Ninomiya, Z. B. Dong, Y. Suzuki, and J. Koketsu, Fuel **79**, 449 (2000).
[14] X. Cheng, J. Mol. Struct.: THEOCHEM **731**, 89 (2005).
[15] O. Kikuchi, Y. Hondo, K. Morihashi, and M. Nakayama, Bull. Chem. Soc. Jpn. **61**, 291 (1988).
[16] P. H. Kasai and D. McLeod, J. Am. Chem. Soc. **94**, 720 (1972).
[17] G. Amaral, K. Xu, and J. Zhang, J. Chem. Phys. **114**, 5164 (2001).
[18] K. S. Xu, G. Amaral, and J. S. Zhang, J. Chem. Phys. **111** 6271 (1999).
[19] W. D. Zhou, Y. Yuan, S. P. Chen, and J. S. Zhang, J. Chem. Phys. **123**, 054330 (2005).
[20] Y. Song, X. F. Zheng, M. Lucas, and J. S. Zhang, Phys. Chem. Chem. Phys. **13**, 8296 (2011).
[21] Y. Song, M. Lucas, M. Alcaraz, J. S. Zhang, and C. Brazier, J. Chem. Phys. **136**, 044308 (2012).
[22] J. S. Zhang, M. Dulligan, and C. Wittig, J. Phys. Chem. **99**, 7446 (1995).
[23] T. J. Wallington, H. Egsgaard, O. J. Nielsen, J. Platz, J. Sehested, and T. Stein, Chem. Phys. Lett. **290**, 363 (1998).
[24] B. Negru, S. J. Goncher, A. L. Brunsvold, G. M. P. Just, D. Park, and D. M. Neumark, J. Chem. Phys. **133**, 074302 (2010) .
[25] X. Lories, J. Vandooren, and D. Peeters, Phys. Chem. Chem. Phys. **12**, 3762 (2010).
[26] L. K. Madden, L. V. Moskaleva, S. Kristyan, and M. C. Lin, J. Phys. Chem. A **101**, 6790 (1997).
[27] A. M. Mebel and A. Landera, J. Chem. Phys. **136**, 234305 (2012).

DOI:10.1063/1674-0068/27/06/621-627